A GPS-Tracked Surf Zone Drifter*

W. E. SCHMIDT, B. T. WOODWARD, K. S. MILLIKAN, AND R. T. GUZA

Integrative Oceanography Division, Scripps Institution of Oceanography, La Jolla, California

B. RAUBENHEIMER AND STEVE ELGAR

Woods Hole Oceanographic Institution, Woods Hole, Massachusetts

ABSTRACT

A drifter designed to measure surf zone circulation has been developed and field tested. Drifter positions accurate to within a few meters are estimated in real time at 0.1 Hz using the global positioning system (GPS) and a shore-to-drifter radio link. More accurate positions are estimated at 1 Hz from postprocessed, internally logged data. Mean alongshore currents estimated from trajectories of the 0.5-m-draft drifters in 1–2-m water depth agree well with measurements obtained with nearby, bottom-mounted, acoustic current meters. Drifters deployed near the base of a well-developed rip current often followed eddylike paths within the surf zone before being transported seaward.

1. Introduction

Surf zone circulation, which is driven primarily by breaking waves (Longuet-Higgins 1970), transports sediments, pollutants, and swimmers. Changes in wave breaking owing to variations in wave height and direction along curving coastlines, irregular bathymetry, and man-made structures are believed to cause complex surf zone circulation, including rip currents and mean alongshore currents that can change direction both across the surf zone and along a depth contour (Shepard and Inman 1950). Large numbers of fixed, single-point current meters would be required to resolve spatially complex circulation. Drifters often have been used to complement fixed current meters in the deep ocean (e.g., McPhaden et al. 1991) and on the continental shelf (e.g., Davis 1985). Here, laboratory and field tests of a surf zone drifter and results from a deployment near a rip current are described.

2. Surf zone drifter design

High impacts from breaking waves and the tendency to ''surf'' shoreward precluded the use of an existing nearshore drifter constructed of canvas mounted on a fiberglass frame (George and Largier 1996). Instead, an impact-resistant body of tubular polyvinyl chloride (PVC) is ballasted for nearly complete submergence and a strong righting moment (Fig. 1). A PVC disc at the bottom of the body tube dampens the vertical response of the drifter, allowing broken and near-breaking waves to pass over without rapidly pushing the drifter ashore. Heave and roll of the drifter, which can degrade GPS position estimates by causing large, rapid deviations of the antenna orientation from vertical, are reduced by the damping plate and by the vertical separation of the centers of buoyancy and mass.

Each drifter records GPS pseudorange and carrier phase data at 1 Hz for postprocessing, and transmits this information to shore at 10-s intervals for real-time differential GPS (DGPS) tracking and partial data backup (Fig. 2). The telemetry range is about 5000 m for a shore antenna elevation of 10 m. Battery storage limits the deployment duration to 24 h.

3. GPS considerations

The small spatial [$O(5$ m)] and short temporal [$O(1$ min)] scales of interest in surf zone circulation are resolved with GPS techniques used in coastal and nearship drifters [e.g., real-time DGPS, 3–5-m accuracy (George and Largier 1996) and carrier phase postprocessing, <1-m accuracy (Doutt et al. 1998)]. However, in the surf zone, submergence by breaking and broken waves prevents the reception of GPS signals, and upon surfacing and reacquiring signal there is a delay in es-
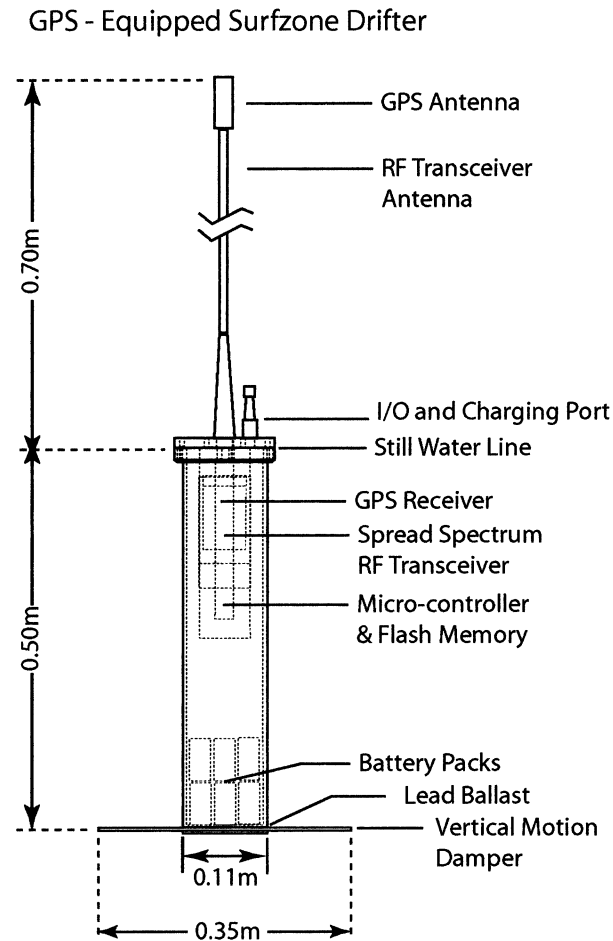
GPS - Equipped Surfzone Drifter

FIG. 1. Schematic of the surf zone drifter. Surface piercing antennae for receiving GPS signals and for radio-frequency (RF) communication with shore are molded permanently to the drifter top cap. A six-pin port, also integral to the top cap, permits programming and data downloading (I/O), and battery charging without opening the drifter package.

timating GPS parameters (3 s for pseudorange and 16 s for carrier phase, for the receiver used). Data gaps (usually less than 1 min) are filled using linear interpolation. The amount of interpolation required varies. In a 72-min deployment entirely within the surf zone, a drifter acquired about 54 min of data (75% data return rate) with 35 data gaps (maximum 1.5 min and mean 0.5 min). Seaward of the surf zone, data return rates are usually above 95%.

Velocity estimates obtained by first-differencing position data contain errors associated with the GPS solution. Absolute GPS position error (i.e., deviation from the true location) can be estimated by the sum of the standard deviations of the measurement and model errors associated with the position solution (Langley 1999). By this method, root-mean-square (rms) absolute errors are approximately 0.2 m when the present receiver is stationary and can be 1 m or more when deployed in the surf. These errors do not necessarily trans-

late into velocity estimate errors, however, because some of the largest measurement and modeling errors (e.g., satellite constellation geometry and atmospheric delay) typically change little from second to second.

Relative GPS position errors (i.e., errors in the distance and bearing between successive GPS positions) are a good measure of 1-Hz, first-difference velocity estimate accuracy. The rms relative errors are approximately 0.0007 m when this receiver is stationary but are difficult to quantify when the receiver is in motion. However, field results described below suggest that errors associated with the GPS solution are not large enough to corrupt typical mean flow estimates.

4. Laboratory and field tests

a. Laboratory tests

The water-following characteristics of the drifter were investigated in the wave and wind channel located in the Scripps Institution of Oceanography (SIO) Hydraulics Laboratory. The 44.5-m-long, 2.4-m-wide, and 2.4-m-high covered channel has a fan-actuated wind intake and hydraulically driven wave paddle at one end.

Drifter performance can be degraded by the rectification of oscillatory wave motions and by windage. Rectification can occur because the drifter behaves as a damped, nonlinear oscillator forced by buoyancy, flow drag forces, and pressure gradients (Davis 1985). For example, if the area submerged or vertical tilt of the drifter (and hence drag) depends on the wave phase, the mean drifter velocity may be nonzero even for a zero-mean orbital velocity. Wave rectification effects were estimated as the difference between mean drifter velocities and mean acoustic Doppler velocimeter (ADV) velocities measured 0.21 m below the mean water surface at one location along the channel centerline, near where the drifter was released. For no wind and mechanically generated, nonbreaking waves of 0.3-m height and 10-s period in 1-m water depth (rms oscillatory velocity 35 cm s^{-1}, and cross-shore velocity skewness and asymmetry of 0.12 and 0.17, respectively), the drifter velocity attributed to wave rectification was less than the accuracy of the ADV (± 1 cm s^{-1}). Mechanical limitations precluded tests with breaking waves.

Windage effects in 1-m water depth were assessed by comparing velocities obtained with two drifters, one with and one without surface piercing features (George and Largier 1996). The velocity difference attributed to wind slip, about 1 cm s^{-1} per 100 cm s^{-1} of near-surface (0.5-m elevation) wind speed, is similar to estimates based on a simple model (Murray 1975) (Fig. 3). The model results and observations are for a flat sea surface and thus do not include the modification of wind by waves that could be important in the surf zone.

b. Field tests

The drifters were observed in the surf zone over a wide range of breaking wave heights (0.3–2.0 m). Video
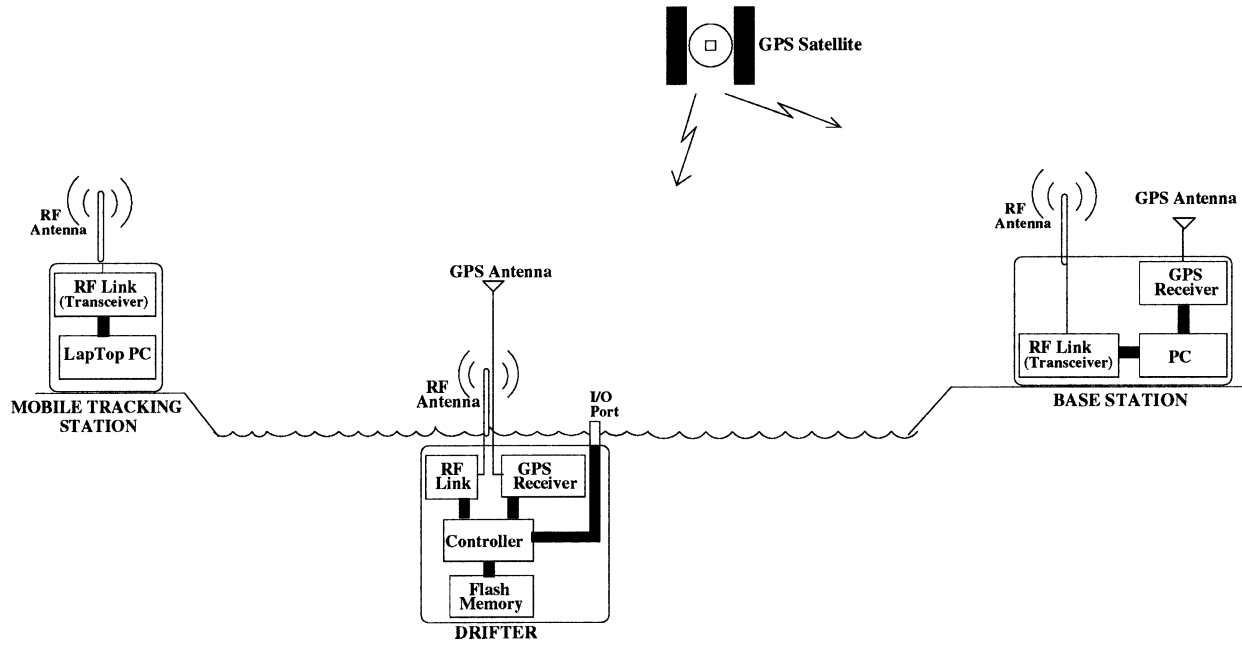
FIG. 2. Drifter system schematic. The base station performs DGPS and datalogging functions, and can serve a fleet of 10 drifters. A mobile tracking station monitors drifter DGPS positions in real time.

records, collected from 10 m above the water surface, typically showed less than 1-m horizontal displacement (often oblique to wave normal) owing to the passage of individual bores or breaking waves. A shoreward mass flux is associated with breaking waves and bores, but by design, bores and breaking waves pass over the drifters. Dye and water-filled balloons were released with a drifter to investigate drifter motions in breaking waves.
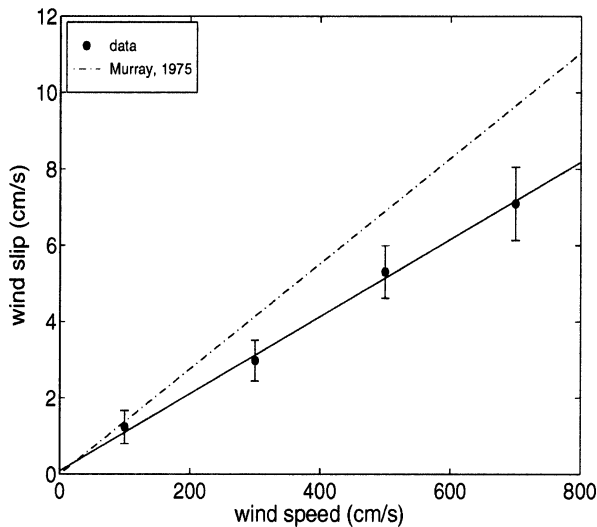

FIG. 3. Wind slip (the difference in the velocity of drifters with and without surface piercing elements) vs wind speed measured 0.5 m above the mean water level. The filled circles and vertical bars represent the mean ± 1 std dev of 10 observations at each wind speed. The solid line is the least squares fit to the mean observations (slope 0.01), and the broken line is the prediction (Murray 1975).

Dye was released 5 times near the sea surface at the seaward edge of the surf zone, with incident wave heights between 0.5 and 0.9 m. Small amounts of the dye were entrained in, and transported shoreward by, every breaking wave or bore, resulting in a faint streak of dye stretching onshore from the area of highest dye concentration to the shoreline. However, the seaward edge of the dye could be advected seaward (out of the surf zone) or shoreward by water movements not directly associated with the passage of individual bores. In every case, the drifter moved offshore or onshore with the seaward edge of the dye, and remained in or near the area of highest dye concentration (as observed visually). Similar results were observed with water-filled balloons. In three releases, the smaller balloons (0.2-m diameter) always advected shoreward with bores, while the larger balloon (0.5-m diameter) was not entrained in bores and moved offshore or onshore, usually in conjunction with the drifter. Differential cross-shore velocities, estimated from the drifter–large balloon cross-shore separation after a few minutes, ranged from 10 to less than 1 cm s^{-1}. These dye and balloon tests suggest that the drifter cross-shore velocities are similar to those of near-surface water particles that are not entrained in bores.

In another test, drifter velocities (computed by first-differencing time series of 1-Hz drifter positions) were compared with velocities observed with two nearby ADVs that sampled within the lower meter of the water column (Fig. 4). Pairs of drifters were released repeatedly in 1–2-m water depth upcurrent of the ADV and retrieved downcurrent of the ADV over roughly 2.5 h
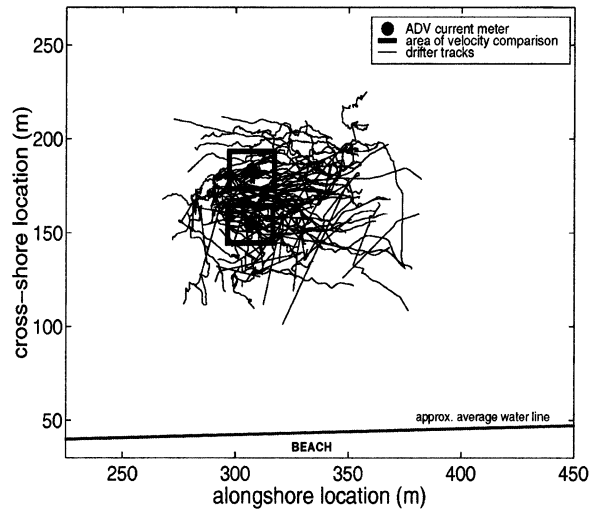
FIG. 4. Drifter trajectories (thin curves) and ADV current meter locations (filled circles). The boxes show the area of the drifter–ADV comparisons. Approximately half of the trajectories are omitted for clarity.

FIG. 5. Drifter (8 min) and ADV (10 min) velocity spectra (20 degrees of freedom) approximately 10 m seaward of the surf zone.

on each of 5 days during the period 4–11 October 2000. No rip currents were observed visually in the deployment area (50–150 m north of the SIO pier, 32.86°N, 117.25°W). Wind speeds measured at the end of the pier, 20.2 m above mean lower low water and 100 m offshore of the experiment site, were moderate during the deployments, averaging 190 cm s^{-1} and ranging from 0 to 800 cm s^{-1}. Significant wave heights, estimated using data from pressure sensors collocated with the ADV, ranged from 0.3 to 1.2 m. Breaking wave heights (estimated from video) reached 1.5 m. Drifters were released both within and seaward of the surf zone, depending on tide level and wave height.

Velocity power spectra obtained from a drifter trajectory and a concurrent ADV record are similar in shape and magnitude below about 0.3 Hz (Fig. 5), as expected from linear wave theory. Consistent with the expected refraction of swell–sea waves (frequencies 0.05–0.20 Hz) to near-normal incidence, spectral levels of alongshore velocity are an order of magnitude lower than cross-shore velocity levels. Alongshore and cross-shore drifter velocity spectra contain peaks at roughly 0.4 Hz that are attributed to drifter heave and roll. Drifter trajectories (and the associated drifter velocities) shown
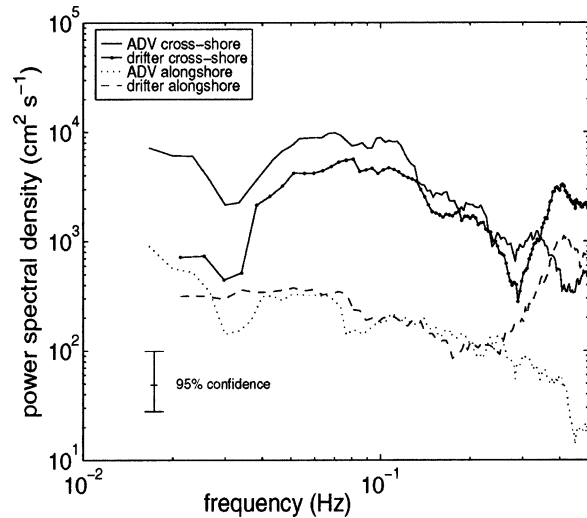
below are low-pass filtered (the cutoff frequency is 0.05 Hz).

Mean velocities were compared only for the time periods (of at least 30 s) in which a drifter was within about 10 m of an ADV (Fig. 4). Drifter and ADV alongshore means are significantly correlated (95% confidence level), both within and seaward of the surf zone (Fig. 6a and Table 1). The rms differences between drifter and ADV alongshore currents are less than 10 cm s^{-1} ($<1/3$ of rms alongshore velocities) and are not strongly dependent on flow speed for the conditions considered. Deployment-averaged ADV and drifter alongshore velocities differ by less than 3 cm s^{-1}. The ADV and drifter mean cross-shore flows are weak seaward of the surf zone (Fig. 6b), with rms values less than 5 cm s^{-1}. Within the surf zone, the near-bottom ADVs measure primarily offshore-directed mean flows (undertow), whereas the near-surface flows measured by the 0.5-m-draft drifters are predominantly onshore (Fig. 6b). These comparisons are consistent with surf zone field observations of weakly vertically sheared alongshore currents (Garcez Faria et al. 1998) and strongly vertically sheared cross-shore currents (Garcez Faria et al. 2000).

TABLE 1. Comparison of alongshore and cross-shore velocity statistics observed with drifters and nearby ADVs within and seaward of the surf zone (Fig. 4). "Corr" is the correlation between ADV and drifter means (shown in Fig. 6), "ADV" and "drifter rms" are the root-mean-squares of their respective mean velocities, "Rms diff" is the root-mean-square difference between ADV and drifter means, and the last two columns are averages of the means.

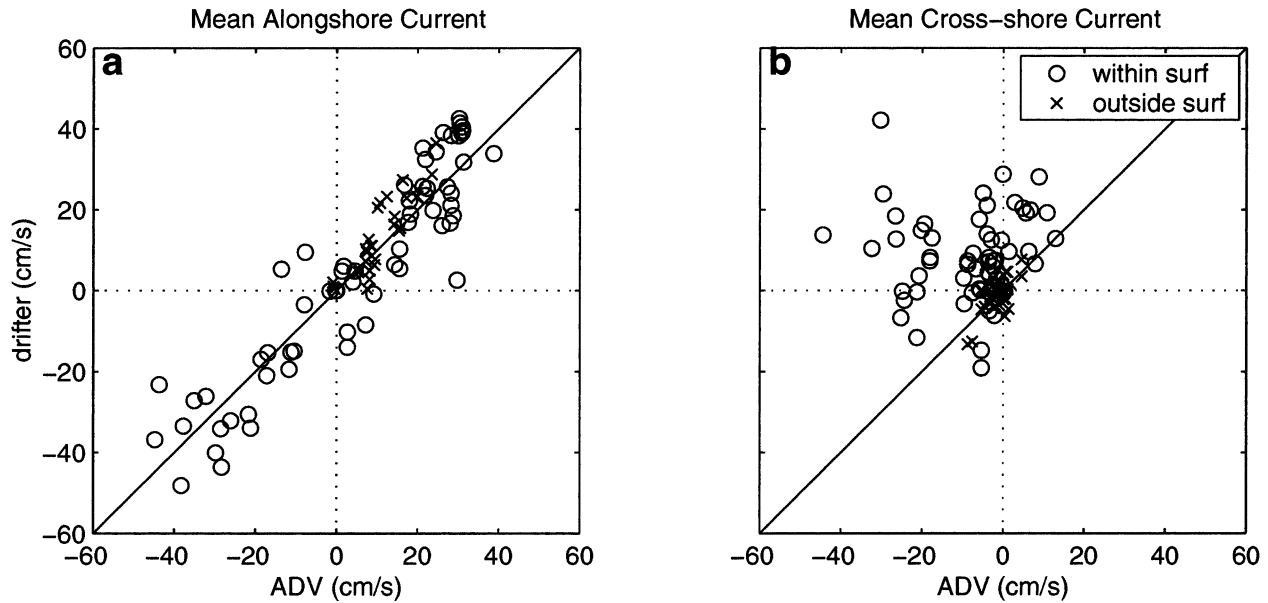| Velocity (location)	Corr	ADV rms (cm s^{-1})	Drifter rms (cm s^{-1})	Rms diff (cm s^{-1})	ADV avg (cm s^{-1})	Drifter avg (cm s^{-1})
Alongshore (surf zone)	0.95	26.8	26.4	9.6	4.4	3.9
Alongshore (seaward)	0.89	12.4	16.3	4.7	10.5	13.2
Cross-shore (surf zone)	−0.01	15.9	13.5	16.0	−6.1	7.2
Cross-shore (seaward)	0.71	3.2	4.5	3.1	−1.3	−1.0

FIG. 6. Mean currents observed with drifters vs mean currents observed with fixed current meters (ADVs): (a) alongshore (north is positive) and (b) cross-shore (onshore is positive). The sloped solid lines correspond to perfect agreement. Surf zone location was determined from video images. See Table 1 for statistics.

5. A rip current deployment

Three drifters were deployed repeatedly over a 3-h period on 25 July 2000 near a frequently occurring rip current (a strong, narrow, seaward-directed flow that advected foam and surfers offshore) located 400 m south of the SIO pier (Shepard and Inman 1950). The deployment spanned a neap low tide with about 0.2-m mean water level fluctuation. At the pier end ($\approx$8 m water depth), the significant wave height ranged from 0.7 to 0.9 m and winds ranged from 200 to 300 cm s^{-1}
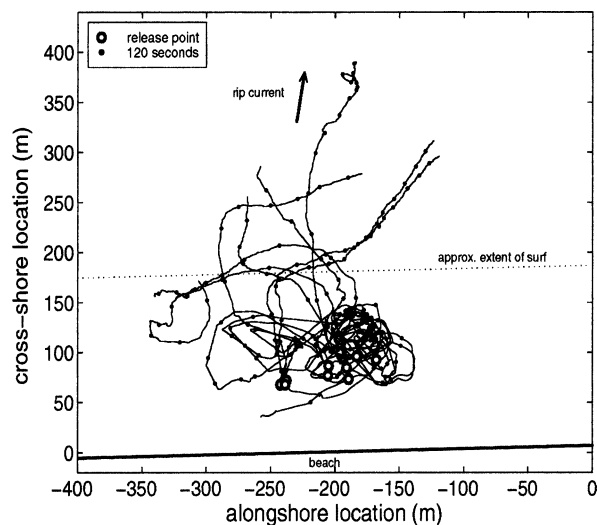

FIG. 7. Trajectories of drifters released (locations shown with large circles) near the base of a rip current. The small filled circles on each trajectory indicate 120-s intervals.

onshore. The drifters were released in approximately 1.5-m water depth near the shoreward end of the rip current. Of 12 individual releases, 2 drifters beached within 1 min (not shown), 1 beached after 72 min, and 9 were retrieved seaward of the surf zone (Fig. 7). The alongshore extent of the seaward-directed trajectories is $O(100$ m).

Surf zone eddies associated with rip currents have been predicted theoretically and numerically (Peregrine 1998; Chen et al. 1999; Svendsen et al. 2000), and noted in field and laboratory observations (Shepard et al. 1941; Komar 1971; Sonu 1972; Dronen et al. 1999). The paths of drifters released during the first 102 min are consistent with a clockwise (CW) rotating eddy with vorticity (Ω) about -0.03 s^{-1} centered near (-175, 100 m) (Fig. 8, trajectories c, d, and e, in addition to two interim trajectories that are not shown). Subsequent releases suggest a CW eddy in approximately the same location (Fig. 9, trajectories a and b), and also a counterclockwise (CCW) rotating eddy, with Ω about 0.02 s^{-1}, centered near (-250, 100 m) (Fig. 9, trajectories a, b, and c). The vorticity is estimated by assuming solid-body rotation, so that $\Omega = 2\omega$, where angular velocity $\omega = 2\pi/T$, and T is the observed revolution period in seconds.

The well-developed rip current and CW eddy persisted for at least 2 h. However, the paths of drifters that exited the surf zone (trajectories a, b, d, and e in Fig. 8), assumed to delineate the rip current position, were temporally variable. Trajectories a and b, initially shore-normal, turned sharply north upon exiting the surf zone. Trajectories d and e, roughly 120 min later, were
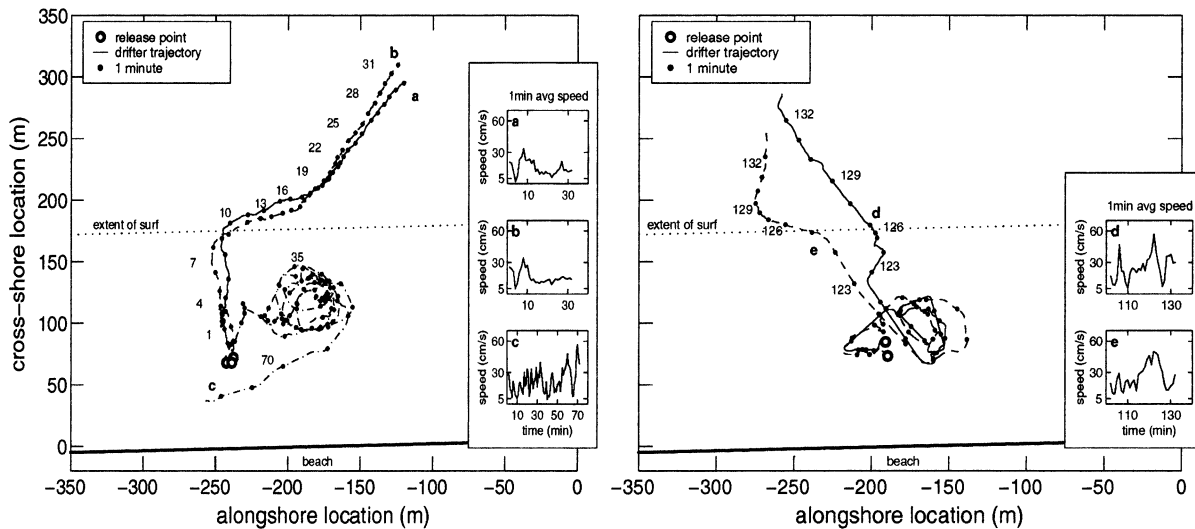
FIG. 8. (left) Trajectories of three drifters deployed at time = 0 min, within a few meters of each other (large circles). Time (min) is indicated along the trajectories, and the inset panel shows mean (1 min) speed vs time. Drifters a (solid) and b (dashed) immediately moved offshore in the rip current, at speeds reaching about 30 cm s^{-1}. Drifter c (dot–dash) was entrained in a CW eddy for about 50 min, making about seven revolutions. The maximum mean speed of c (about 55 cm s^{-1}) was directed roughly alongshore. (right) Trajectories of two drifters [d (solid) and e (dashed)] released at time = 102 min. Both drifters made about two CW revolutions and then exited the surf zone. Maximum mean speeds (about 50 cm s^{-1}) occur as the drifters leave the eddy and are directed roughly offshore. Drifters in the CW eddy (c, d, and e) rotated at roughly one revolution every 7 min.

oblique to the south. In marked contrast, the seaward extent of the last trajectories is minimal (Fig. 9). The variable rip current structure and the apparent transition (over a roughly 1-h period) from a well-developed rip current (Fig. 8) to a circulation lacking a narrow, seaward-directed jet (Fig. 9) may be related to a hydrodynamic instability of the rip current [cf. Figs. 8 and 9 with the numerically predicted evolution in Plate 3b of Chen et al. (1999)] or to an instability of the alongshore current (Smith and Largier 1995). Variations in tidal

and wind-driven currents could have also contributed to the rip current variability. A fleet of 10 drifters under construction will permit more extensive sampling.

6. Conclusions

A surf zone drifter has been developed and tested. Mean alongshore velocities from drifters and nearby fixed current meters within the surf zone agree well (correlation 0.95 and rms differences of 10 cm s^{-1}).
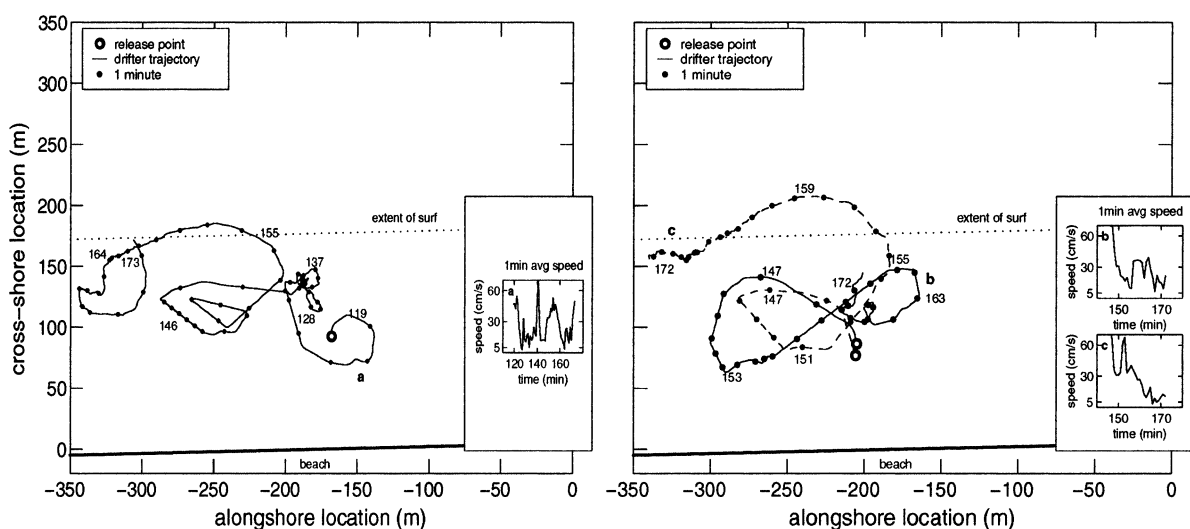

FIG. 9. Trajectories of the last three drifters, deployed at (left) time = 118 min and (right) time = 145 min. These three trajectories had the highest mean speeds (about 70 cm s^{-1}, directed roughly alongshore) and suggest a CCW eddy centered near (−250, 100 m) and a CW eddy (also see Fig. 8) centered near (−175, 100 m).

Drifters deployed near a rip current often followed eddylike trajectories before being advected seaward of the surf zone.

REFERENCES

Chen, Q., R. A. Dalrymple, J. T. Kirby, A. B. Kennedy, and M. C. Haller, 1999: Boussinesq modeling of a rip current system. *J. Geophys. Res.,* **104,** 20 617–20 637.

Davis, R. E., 1985: Drifter observations of coastal surface currents during CODE: The method and descriptive view. *J. Geophys. Res.,* **90,** 4741–4755.

Doutt, J. D., G. V. Frisk, and H. Martell, 1998: Using GPS at sea to determine the range between a moving ship and a drifting buoy to centimeter-level accuracy. *Proc. Oceans '98,* Nice, France, Institute of Electrical and Electronic Engineering, 1344–1347.

Dronen, N., H. Karunarathna, J. Fredsoe, B. M. Sumer, and R. Deigaard, 1999: The circulation over a longshore bar with rip channels. *Proc. Coastal Sediments '99,* Hauppauge, NY, Amer. Soc. Mechanical Engineers, 576–587.

Garcez Faria, A. F., E. B. Thornton, T. P. Stanton, C. V. Soares, and T. Lippmann, 1998: Vertical profiles of longshore currents and related bed shear stress bottom roughness. *J. Geophys. Res.,* **103,** 3217–3232.

——, ——, T. C. Lippmann, and T. P. Stanton, 2000: Undertow over a barred beach. *J. Geophys. Res.,* **105,** 16 999–17 010.

George, R., and J. L. Largier, 1996: Description and performance of finescale drifters for coastal and estuarine studies. *J. Atmos. Oceanic Technol.,* **13,** 1322–1326.

Komar, P. D., 1971: Nearshore cell circulation and the formation of giant cusps. *Geol. Soc. Amer. Bull.,* **82,** 2643–2650.

Langley, R. B., 1999: Dilution of precision. *GPS World,* **5,** 54–59.

Longuet-Higgins, M. S., 1970: Longshore currents generated by obliquely incident seawaves, 1. *J. Geophys. Res.,* **75,** 6790–6801.

McPhaden, M. J., D. V. Hansen, and P. L. Richardson, 1991: A comparison of ship drift, drifting buoy, and current meter mooring velocities in the Pacific South Equatorial Current. *J. Geophys. Res.,* **96,** 775–781.

Murray, S. P., 1975: Trajectories and speeds of wind-driven currents near the coast. *J. Phys. Oceanogr.,* **5,** 347–360.

Peregrine, D. H., 1998: Surf zone currents. *Theor. Comput. Fluid Dyn.,* **10,** 295–309.

Shepard, F. P., and D. I. Inman, 1950: Nearshore water circulation related to bottom topography and wave refraction. *Trans. Amer. Geophys. Union,* **31,** 196–212.

——, K. O. Emery, and E. C. La Fond, 1941: Rip currents: A process of geological importance. *J. Geol.,* **49,** 337–369.

Smith, J. A., and J. L. Largier, 1995: Observations of nearshore circulation: Rip currents. *J. Geophys. Res.,* **100,** 10 967–10 975.

Sonu, C. J., 1972: Field observations of nearshore circulation and meandering currents. *J. Geophys. Res.,* **77,** 3232–3247.

Svendsen, I. A., K. A. Haas, and Q. Zhoa, 2000: Analysis of rip current systems. *Proc. Coastal Eng. 2000,* Sydney, Australia, Amer. Soc. Civil Engineers, 1127–1140.